

The submitted manuscript has been authored by a contractor of the U. S. Government under contract No. W-31-109-ENG-38. Accordingly, the U. S. Government retains a nonexclusive, royalty-free license to publish or reproduce the published form of this contribution, or allow others to do so, for U. S. Government purposes.

LS-218

79396

Fundamental Mode RF Power Dissipated in a Waveguide Attached to an Accelerating Cavity

Y. W. Kang

RF Group
Accelerator Systems Division
Argonne National Laboratory

February 9, 1993

I. Introduction

An accelerating RF cavity usually requires accessory devices such as a tuner, a coupler, and a damper to perform properly. Since a device is attached to the wall of the cavity to have certain electrical coupling of the cavity field through the opening, RF power dissipation is involved. In a high power accelerating cavity, the RF power coupled and dissipated in the opening and in the device must be estimated to design a proper cooling system for the device. The single cell cavities of the APS storage ring will use the same accessories. These cavities are rotationally symmetric and the fields around the equator can be approximated with the fields of the cylindrical pillbox cavity. In the following, the coupled and dissipated fundamental mode RF power in a waveguide attached to a pillbox cavity is discussed. The waveguide configurations are 1) aperture- coupled cylindrical waveguide with matched load termination, 2) short- circuited cylindrical waveguide, and 3) E-probe or H-loop coupled coaxial waveguide. A short-circuited, one-wavelength coaxial structure is considered for the fundamental frequency rejection circuit of an H-loop damper.

II. Coupled Waveguide Modes

Figure 1 shows a pillbox cavity with a cylindrical waveguide attached to it. For TM_{010} mode, fields in the cavity are

$$E_z = \frac{k^2}{j\omega\epsilon} J_0(k_{\rho'}\rho'), \quad H_{\phi'} = k_{\rho'} J_1(k_{\rho'}\rho') \quad (1)$$

where J_n is the n -th order Bessel function of the first kind. The fundamental mode RF power dissipated in the cavity with the fields in equation (1) is

$$P = \iint_{\text{cavity wall}} R_s |H_{\phi'}(\rho', \phi', z)|^2 ds \quad (2)$$

where R_s is the surface resistance of the cavity metal

$$R_s = \sqrt{\frac{\omega\mu}{2\sigma}}. \quad (3)$$

For the cavity input power P_{in} , the fields are

$$E_z = b_n \frac{k^2}{j\omega\epsilon} J_0(k_{\rho'}\rho'), \quad H_{\phi'} = b_n k_{\rho'} J_1(k_{\rho'}\rho')$$

where

$$b_n = \sqrt{\frac{P_{in}}{P}}.$$

The magnetic field in the aperture S_a is assumed to be uniform and ϕ' -directed.

$$\hat{\mathbf{a}}_x H^a \simeq \hat{\mathbf{a}}_{\phi'} H_{\phi'} \quad (4)$$

In a circularly cylindrical waveguide, the mode functions are

$$\begin{aligned} \mathbf{H}_{np}^{TM} &= \hat{\mathbf{a}}_{\rho} \frac{jn}{\rho} J_n(k_{\rho}\rho) e^{jn\phi} e^{-jk_z z} \\ &\quad - \hat{\mathbf{a}}_{\phi} k_{\rho} J'_n(k_{\rho}\rho) e^{jn\phi} e^{-jk_z z} \end{aligned} \quad (5)$$

for TM modes, where

$$k_z^2 = \sqrt{k^2 - k_{\rho}^2}, \quad k_{\rho} = \frac{x_{np}}{a}$$

and

$$\begin{aligned}
\mathbf{H}_{np}^{TE} = & -\hat{\mathbf{a}}_\rho \frac{k_z k_\rho}{\omega \mu} J'_n(k_\rho \rho) e^{jn\phi} e^{-jk_z z} \\
& -\hat{\mathbf{a}}_\phi \frac{jk_z n}{\omega \mu \rho} J_n(k_\rho \rho) e^{jn\phi} e^{-jk_z z} \\
& +\hat{\mathbf{a}}_z \frac{k^2 - k_z^2}{j\omega \mu} J_n(k_\rho \rho) e^{jn\phi} e^{-jk_z z}
\end{aligned} \tag{6}$$

for TE modes, where

$$k_z^2 = \sqrt{k^2 - k_\rho^2}, \quad k_\rho = \frac{x'_{np}}{a},$$

a is the guide radius, k is the free space wave number, and x_{np} and x'_{np} are the p -th zeros of J_n and J'_n , respectively.

The aperture field can be expressed in a two-dimensional Fourier-Bessel series as

$$\mathbf{H}^a = \sum_{n=0}^{\infty} \sum_{p=1}^{\infty} (c_{np}^{TM} \mathbf{h}_{np}^{TM} + c_{np}^{TE} \mathbf{h}_{np}^{TE}) \tag{7}$$

where \mathbf{h}_{np} are the normalized mode vectors with

$$\iint_{\text{cross section}} |h_{np}|^2 ds = 1. \tag{8}$$

From equation (7), the Fourier expansion coefficients are found as

$$c_{np} = \int_0^a \int_0^{2\pi} \mathbf{H}^a(\rho, \phi) \cdot \mathbf{h}_{np}(\rho, \phi) \rho d\rho d\phi. \tag{9}$$

For the uniform aperture field in equation (4),

$$\mathbf{H}^a = |H^a|(\hat{\mathbf{a}}_\rho \cos\phi - \hat{\mathbf{a}}_\phi \sin\phi). \tag{10}$$

III. Power Dissipation in a Matched Load Terminated Waveguide

For each mode, the dissipated power in the waveguide is the dissipated power in the waveguide wall plus the dissipated power in the matched load. The dissipated power in the load equals the time average power flow through the waveguide. The total power dissipation

$$\begin{aligned}
 P_d &= P_{wall} + P_{load} \\
 &= \int_0^{2\pi} \int_0^{\ell} R_s |H(a, \phi, z)|^2 d\phi dz + R_e \left\{ \int_0^a \int_0^{2\pi} \mathbf{E} \times \mathbf{H}^* \cdot \hat{\mathbf{a}}_z \rho d\rho d\phi \right\} \quad (11)
 \end{aligned}$$

where E and H are the fields inside the waveguide supported by the aperture field in equation (7).

The $np - th$ modal electric field is

$$E_{np} = Z^\omega H_{np}$$

where the wave impedances are given as

$$Z^{\omega, TM} = \frac{E_\rho}{H_\phi} = \frac{k_z}{\omega \epsilon}$$

for TM modes and

$$Z^{\omega, TE} = -\frac{E_\phi}{H_\rho} = \frac{\omega \mu}{k_z}$$

for TE modes. At a frequency below the cut-off for the dominant TE_{11} mode of the waveguide, ignoring the wall loss, all the waveguide modes have purely reactive input impedance. The input impedance of the matched load terminated waveguide at the aperture may be found using the transmission line theory. If the length ℓ of the waveguide is sufficiently long, the resistive component of the input impedance is negligible and, therefore, the time average power flow in the waveguide is negligible.

IV. Power Dissipation in a Short-Circuited Waveguide

In a terminated cylindrical waveguide, the magnetic field wave of the np -th mode is

$$H_{np}(z) = H_{np}^+ e^{-\gamma_{np} z} [1 - \Gamma_{np}(z)] \quad (12)$$

where

$$\Gamma_{np}(z) = \frac{H_{np}^-}{H_{np}^+} e^{2\gamma_{np} z}, \quad (13)$$

the propagation constant

$$\gamma = \alpha + j\beta,$$

and H^+ and H^- are the incident and the reflected waves, respectively. In a short-circuited waveguide, $H^-/H^+ = 1$ at the short $z = \ell$. The total power lost in the waveguide section is the power dissipated on the waveguide wall plus the power dissipated on the short.

$$\begin{aligned} P_d &= P_{wall} + P_{short} \\ &= \int_0^{2\pi} \int_0^\ell R_s |H(a, \phi, z)|^2 d\phi dz + \int_0^a \int_0^{2\pi} R_s |H(\rho, \phi, \ell)|^2 \rho d\rho d\phi. \end{aligned} \quad (14)$$

At a frequency below the cut-off of the waveguide mode, the modal field evanesces rapidly and the dissipated power on the short can be ignored if the length ℓ is sufficiently long.

V. Power Dissipation in a Coaxial Transmission Line Section

Figures 2(a) and 2(b) show the coaxial transmission line attached to a cavity through a probe and a loop, respectively. The current induced on the probe is

$$I = \frac{\partial}{\partial t} \iiint_{probe} \epsilon_o E dv \simeq j\omega\epsilon_o AE \quad (15)$$

where A is the probe surface area, and the voltage induced on the loop is

$$V = \frac{-\partial}{\partial t} \iint_{loop} \mu_o \mathbf{H} \cdot d\mathbf{s} \simeq -j\omega\mu_o SH \quad (16)$$

where S is the area of the loop. The coaxial transmission line has a diameter much less than a wavelength and thus coupling of the TM and TE waveguide modes will be ignored. In the coaxial line, only a TEM mode will be excited with no frequency limit. For a short-circuited coaxial transmission line section, the standing wave fields are

$$\mathbf{E} = \hat{\mathbf{a}}_\rho E_o \sin(kz) = \frac{\hat{\mathbf{a}}_\rho V}{\rho \ln(a/b)} \sin(kz) \quad (17a)$$

$$\mathbf{H} = \hat{\mathbf{a}}_\phi \frac{E_o}{\eta} \cos(kz) \quad (17b)$$

where η is the free space wave impedance. The voltage induced on the E -probe is

$$V = Z^{in} I. \quad (18)$$

The total power dissipated in the inner and outer conductor walls and on the short is

$$\begin{aligned} P_d &= P_{ic} + P_{oc} + P_{sc} \\ &= \int_0^{2\pi} \int_0^\ell R_s (|H_\phi(b, \phi, z)|^2 + |H_\phi(a, \phi, z)|^2) d\phi dz \\ &\quad + \int_b^a \int_0^{2\pi} R_s |H_\phi(\rho, \phi, \ell)|^2 \rho d\rho d\phi. \end{aligned} \quad (19)$$

Note that, if P_{sc} is ignored, the power dissipation is inversely proportional to the conductor radius of the coaxial structure for a fixed characteristic impedance Z_o .

VI. Results

In the following, the cases of the cavity to waveguide power coupling described above are discussed with computation results. A cylindrical pillbox cavity whose TM_{010} resonance occurs at $352MHz$ is used in the computation. The radius and the height of the pillbox are $0.325m$ and $0.365m$, respectively. $100KW$ of cavity input power is used.

Transverse magnetic modes have magnetic fields closed in the transverse plane. For equation (9), results show that only the TE_{1p} modes are excited in the waveguide due to the aperture field \mathbf{H}^a . The modal power distribution of the dissipated power in the waveguide is shown in Table 1. The cumulative power dissipation along the axis of the $8cm$ radius waveguide is shown in Figure 3. The power dissipation versus the diameter of the attached waveguide is shown in Figure 4. The waveguide is terminated with a resistive load which is assumed to be matched for all waveguide modes. For TE_{11} mode, the attenuation constant of the $8cm$ radius waveguide is $\alpha = 21.8 \text{ Nepers/m}$. This shows that the RF power at $z = 30 \text{ cm}$ is more than 50 dB below the input power. Therefore, the time average power flow through the waveguide can be ignored.

If the guide length $L > 0.1m$ and the aperture radius $r < 8cm$, from Figure 3, the power dissipations on the short and on the wall due to the reflected field become negligible. Thus, the power dissipation in a short-circuited cylindrical waveguide attached to a pillbox cavity must be similar to the results shown in Figure 3.

The power dissipation in a short-circuited 50Ω coaxial transmission line section versus the radius of outer conductor of a coaxial line is shown in Figure 5. The length of the coaxial section is 1λ at $352MHz$ and the characteristic impedance of the line is 50Ω . The result shows that a coaxial line with greater conductor radius dissipates less, as expected. Since TE_{11} can still couple to the coaxial structure, combining the above result with the power dissipation shown in Figure 4, the optimum radius of a coaxial transmission line may be found.

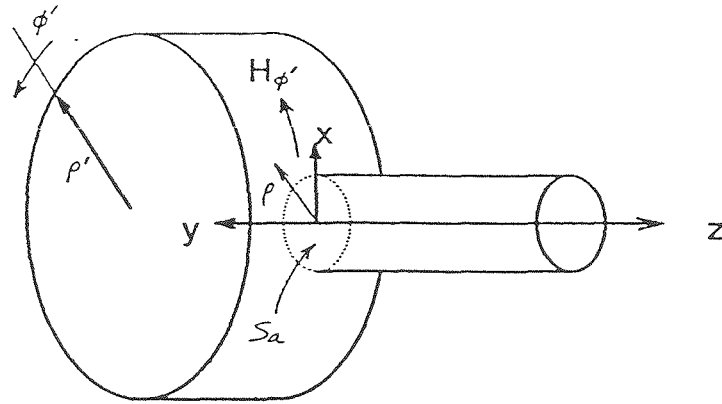
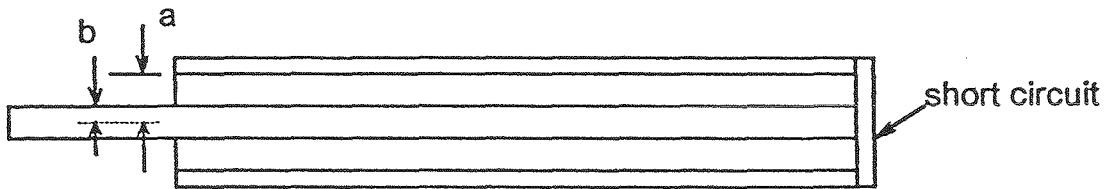
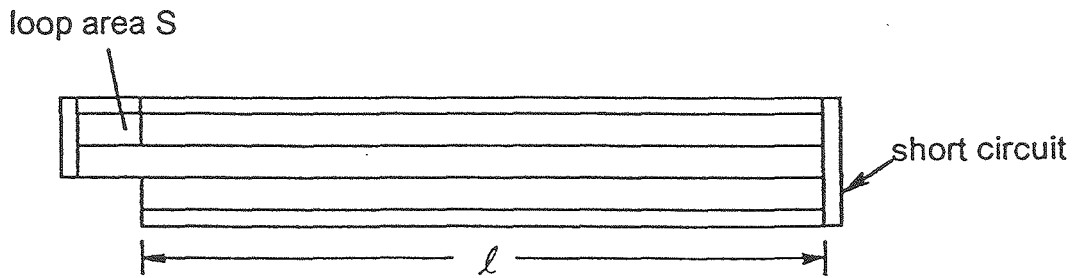


Figure 1. A cylindrical waveguide attached to a pillbox cavity through an aperture



(a) Coaxial transmission line with E-probe



(b) Coaxial transmission line with H-loop

Figure 2. Short-circuited coaxial transmission line sections

Table 1 - Spectral Power Density of Dissipated TE_{1p} Modes
in the Wall of Cylindrical Waveguide vs. Guide Radius

Cavity Input Power=100KW

	r=0.008	r=0.016	r=0.024	r=0.032	r=0.04	r=0.048	r=0.056	r=0.064	r=0.072	r=0.08
p=1	15.2685	33.2464	61.1209	102.203	157.429	227.569	313.74	417.315	540.34	685.253
p=2	0.770316	1.54642	2.32912	3.15064	4.06827	5.13725	6.39718	7.87278	9.57868	11.5238
p=3	0.284867	0.568426	0.852169	1.13673	1.42503	1.72335	2.04014	2.38409	2.76281	3.1824
p=4	0.145061	0.292902	0.440805	0.58879	0.737013	0.886067	1.03724	1.1925	1.35421	1.52482
p=5	0.0922255	0.183247	0.274283	0.365344	0.456446	0.547648	0.639134	0.731289	0.824724	0.920232
p=6	0.0595875	0.12121	0.182868	0.244542	0.306235	0.367953	0.429725	0.491616	0.55378	0.616436
p=7	0.0457792	0.0904809	0.13518	0.179884	0.224597	0.26932	0.314059	0.358827	0.403661	0.448622
p=8	0.0320771	0.0657912	0.0995468	0.133312	0.167085	0.200865	0.234652	0.26845	0.30227	0.336124
p=9	0.027637	0.0542979	0.0809489	0.1076	0.134255	0.160912	0.187575	0.214242	0.240918	0.267607
p=10	0.0199037	0.0411804	0.0625081	0.083845	0.105188	0.126534	0.147884	0.169236	0.190593	0.211958
p=11	0.0187425	0.0365925	0.0544264	0.0722586	0.0900921	0.107927	0.125762	0.143601	0.161442	0.179288
p=12	0.0134889	0.0281528	0.0428777	0.0576138	0.072354	0.087098	0.101844	0.116591	0.13134	0.146092

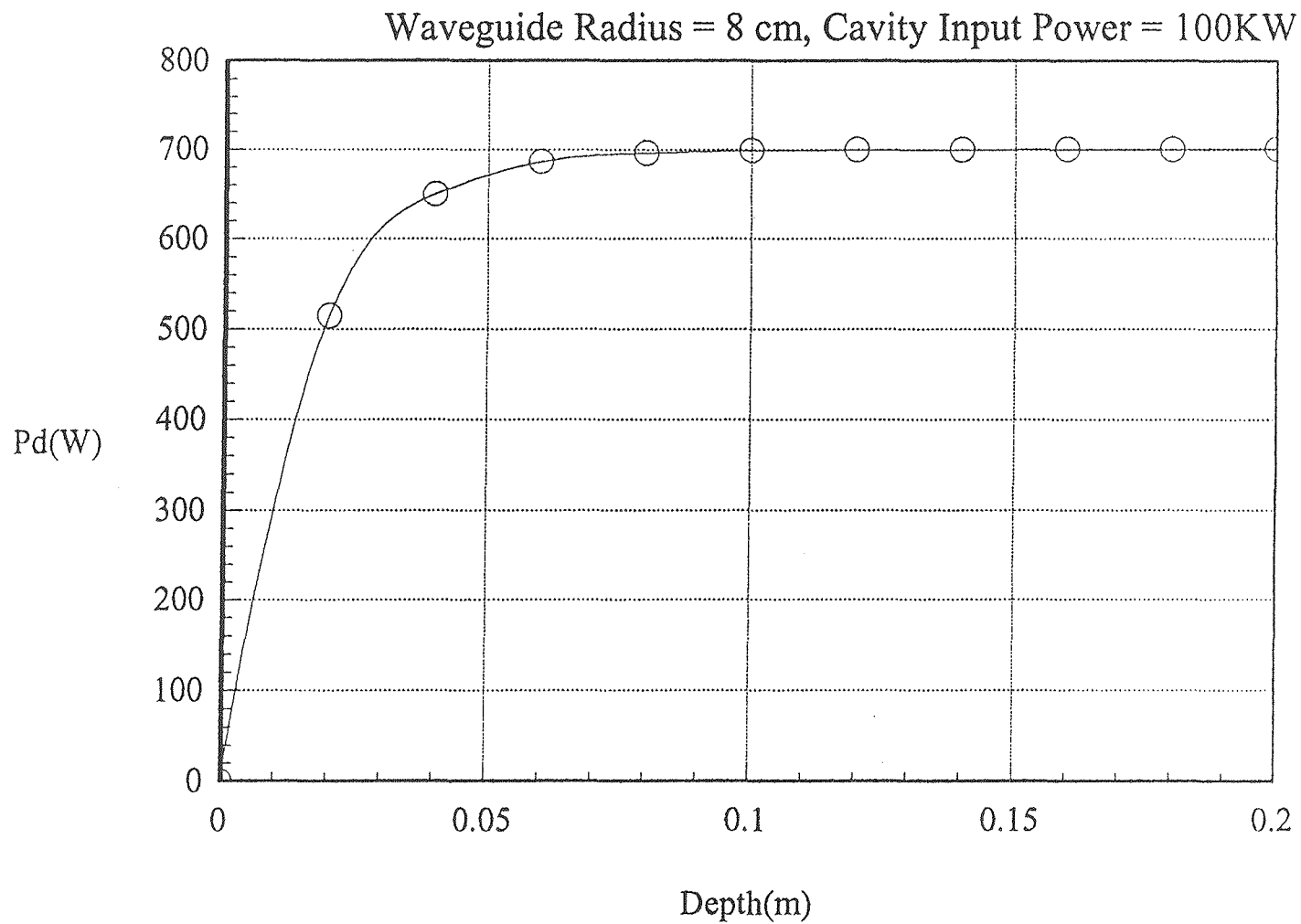


Figure 3. Cumulative Power Dissipation in a Cylindrical Copper Waveguide Wall with Respect to Depth

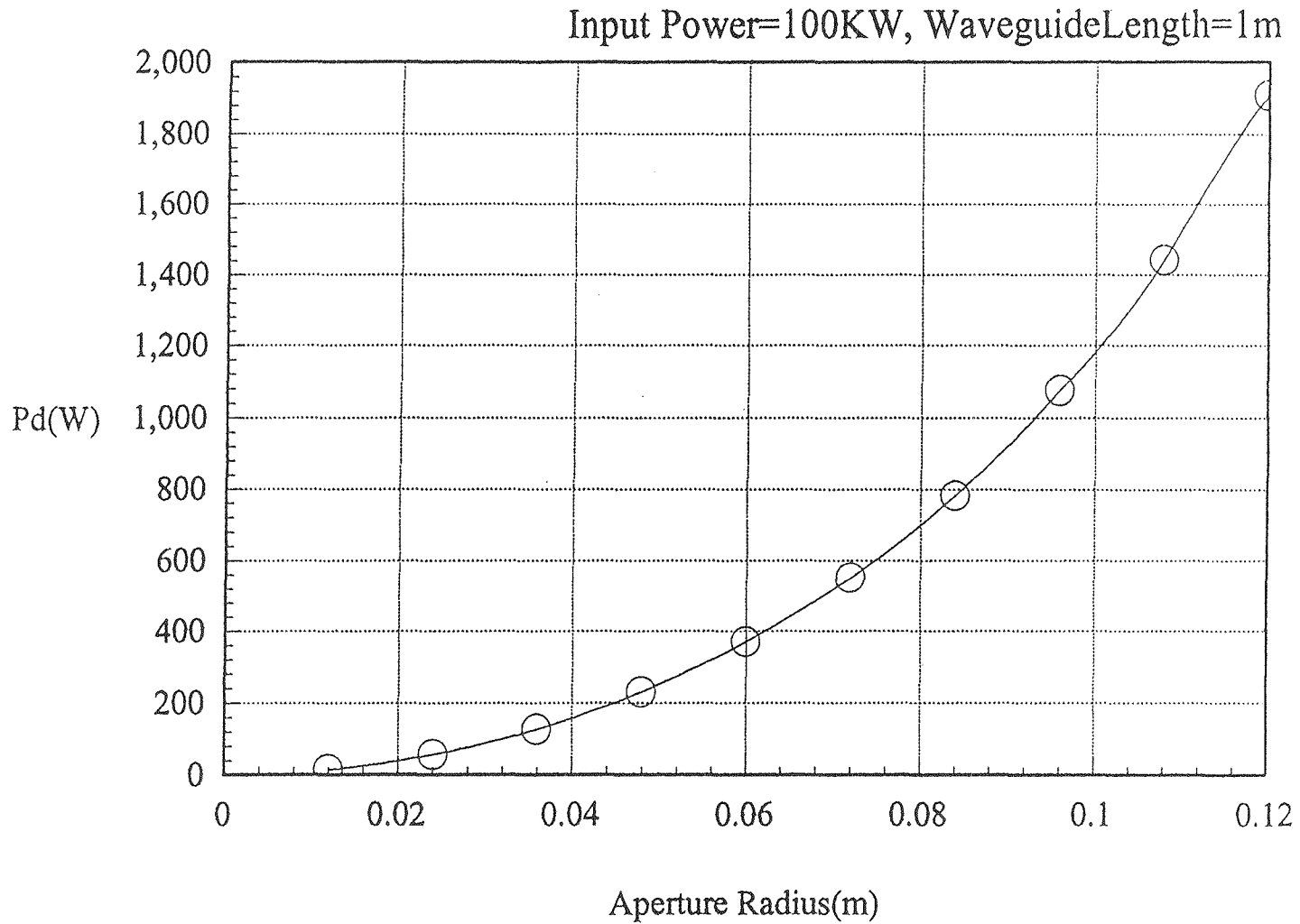


Figure 4. Power Dissipation in a Cylindrical Copper Waveguide Attached to Pillbox Cavity vs. Waveguide Radius

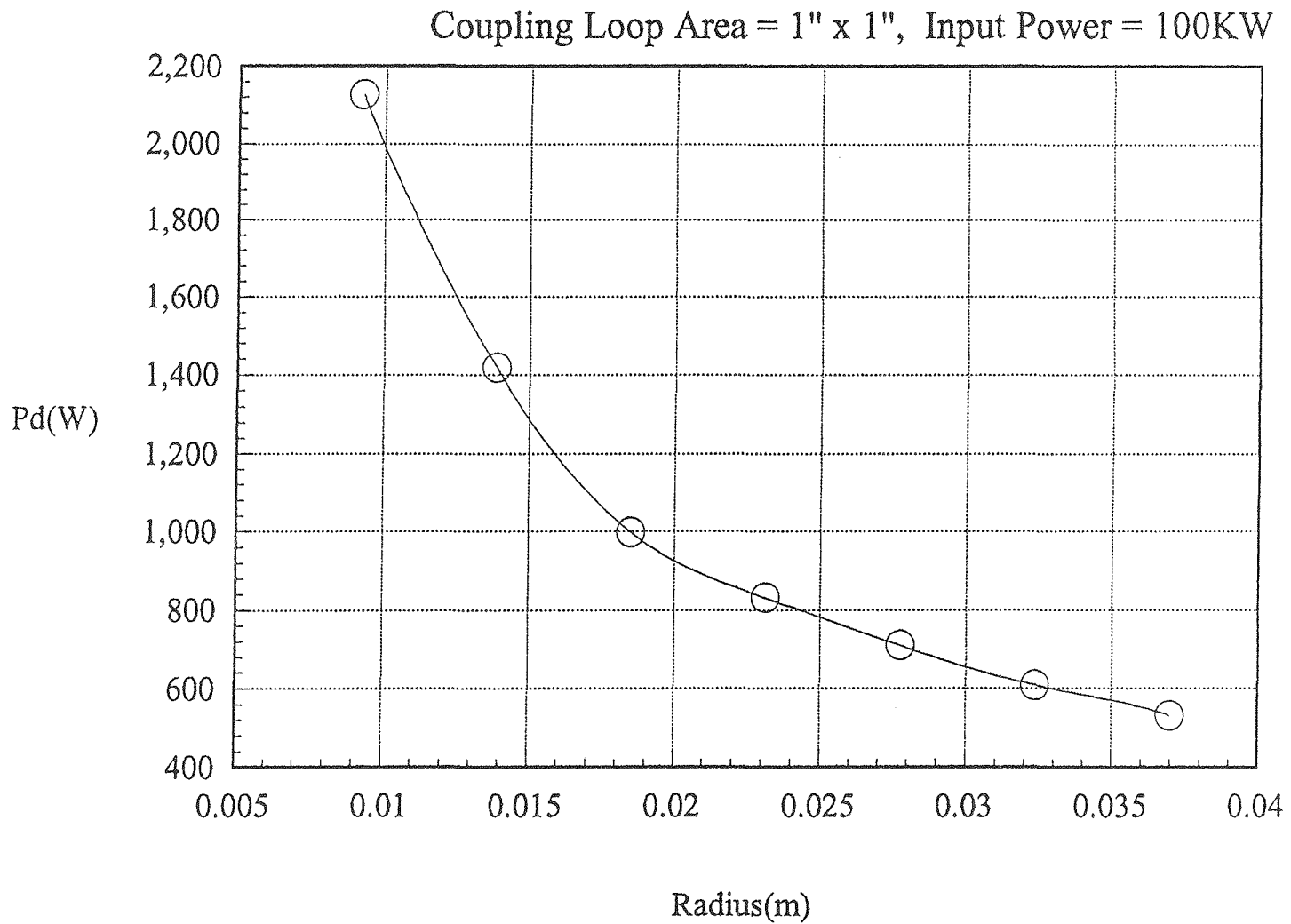


Figure 5. Power Dissipation in a 50Ω 1λ Short-Circuited Coaxial Line Section vs. Outer Conductor Radius